

# Confidence interval estimation of mixed oil length with conditional diffusion model

Yanfeng Yang<sup>1</sup>, Lihong Zhang<sup>1</sup>, Ziqi Chen<sup>1,\*</sup>, Miaomiao Yu<sup>1</sup>, and Lei Chen<sup>2</sup>

<sup>1</sup>East China Normal University, No. 3663, North Zhongshan Road,  
Putuo District, Shanghai, 200062, China

<sup>2</sup>China University of Petroleum (East China), No. 66, West Changjiang  
Road, Huangdao District, Qingdao, 266580, China

\*zqchen@fem.ecnu.edu.cn

June 28, 2024

## Abstract

Accurately estimating the mixed oil length plays a big role in the economic benefit for oil pipeline network. While various proposed methods have tried to predict the mixed oil length, they often exhibit an extremely high probability (around 50%) of underestimating it. This is attributed to their failure to consider the statistical variability inherent in the estimated length of mixed oil. To address such issues, we propose to use the conditional diffusion model to learn the distribution of the mixed oil length given pipeline features. Subsequently, we design a confidence interval estimation for the length of the mixed oil based on the pseudo-samples generated by the learned diffusion model. To our knowledge, we are the first to present an estimation scheme for confidence interval of the oil-mixing length that considers statistical variability, thereby reducing the possibility of underestimating it. When employing the upper bound of the interval as a reference for excluding the mixed oil, the probability of underestimation can be as minimal as 5%, a substantial reduction compared to 50%. Furthermore, utilizing the mean of the generated pseudo samples as the estimator for the mixed oil length enhances prediction accuracy by at least 10% compared to commonly used methods.

**Keywords:** Mixed oil length, Machine learning, Interval estimation, Diffusion model

# 1 Introduction

With the advent of large-diameter and long-distance pipelines, the primary mode of transporting petroleum products has shifted to pipeline transportation [1, 2], which is cost-effective, efficient, and safe [3, 4]. Various types of gasoline, kerosene, jet fuel, diesel, home heating oil, and liquefied gases like butane or propane [5] are conveyed through a shared pipeline without any physical segregation between distinct batches [6]. As illustrated in Figure 1, when different batches move successively through a pipeline, a mixed oil section emerges between them [7], leading to the contamination of the pure products and a substantial compromise in their quality. This results in considerable economic losses due to the degradation in product quality [8]. Therefore, the monitoring mixed oil interface is essential in multi-product pipelines. In particular, accurately calculating the mixed oil length is crucial for optimizing the pipeline network’s scheduling plan to guarantee products meet the required standards [9, 10].

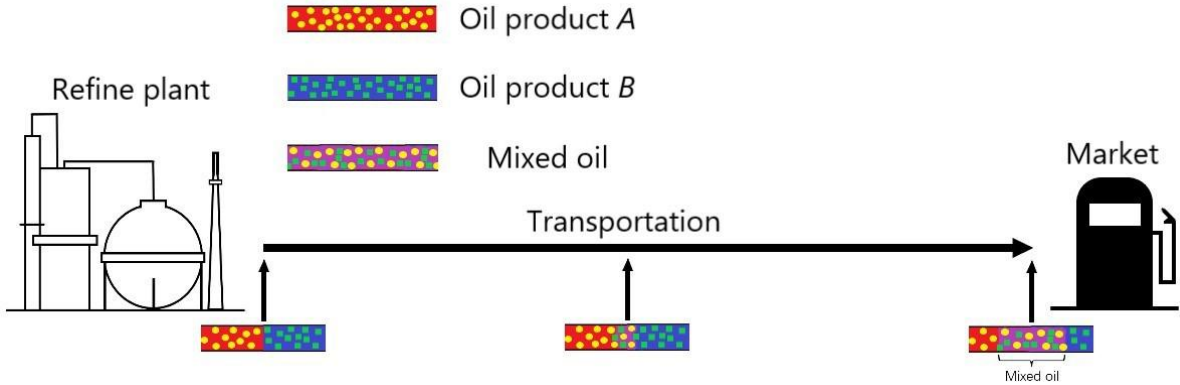


Figure 1: The description of oil mixing phenomenon.

Austin and Palfrey [7] proposed two equations to calculate the length of mixed oil, with empirical parameters estimated from a large-scale industrial dataset. The equations have found extensive practical use, even integrated into renowned commercial software for its convenience in rough estimation. However, its general applicability may be limited since the parameters of the above formula may vary in the different pipelines, environments, etc. [11]. Utilizing the mechanism of convection and diffusion, Wang et al. [12] found that considering the effect of near-wall adsorption can mitigate predictive deviations. By considering the initial mixing, Hamidi [13] introduced a two-dimensional numerical model and achieved more precise results. But implementing such sophisticated methods for real-time prediction of mixed oil length in long-distance industrial pipelines is challenging due to the substantial numerical burden involved. In the fast-paced evolution of advanced optimization technology, researchers are delving into the utilization of machine learning algorithms. Their focus is on harnessing insights from historical

data to construct models that can effectively calculate the length of mixed oil. Partial least squares and deep neural networks have been employed to develop predictive models for mixed oil length [14]. Chen et al. [9] integrated mechanistic models into the gradient boosting decision trees algorithm [15] to develop a dual-driver model for predicting the length of mixed oil. This integration resulted in enhanced prediction accuracy. A serial-parallel residual-based machine learning algorithm, coupled with the Austin-Palfrey formula, has been applied to mitigate the impact of outliers in real pipeline mixed oil data [16]. Utilizing the mechanism model, the Bayesian-Gaussian mixture regression algorithm and the Student’s t mixture regression algorithm were employed to address the prediction of mixed oil length under variational pipeline conditions [17, 18]. Nevertheless, these methods only gave a point estimation, not an interval estimate; that is, the randomness of the sample leads to unrobust point estimation, while the estimate of the confidence interval takes this uncertainty into account.

In real-world scenarios, despite assertions from existing methods about their accuracy in predicting mixed oil length, these models frequently have a high probability (around 50%) of underestimating the mixed oil length. This is primarily due to their failure to account for the statistical variability inherent in the estimated length of mixed oil. In Section 3.4, experiments are carried out to substantiate this phenomenon. Furthermore, the accuracy measure does not differentiate between whether the predicted value is higher or lower than the actual value. To elaborate, consider two predicted values: the first predicted length is  $s$  meters higher than the actual length, and the second predicted length is  $s$  meters lower than the actual value. The RMSE value calculated using (4) for these two predicted values remains identical. When the predicted length exceeds the actual length of the mixed oil, workers can effectively remove the mixed oil from the pipeline. Conversely, if the predicted value falls below the actual length, complete exclusion of the mixed oil is not achievable, leading to increased economic losses.

The pioneering work on the diffusion model can be attributed to Jonathan Ho et al. [19]. Renowned for its ability to accurately learn data distributions with limited samples, the diffusion model has found widespread applications across diverse domains including computer vision [20], natural language processing [21], multimodal modeling [22, 23], and time series processing [24]. Further, some improvements have been made to the original diffusion model, including advancements in sampling acceleration [25, 26], improvements in likelihood maximization [27], and innovations in conditional generation [28]. We learn the distribution of the mixed oil length given pipeline features using the diffusion model. Subsequently, we generate pseudo samples using the learned distribution and use them to construct confidence interval estimation. Our approach takes into account the uncertainty in estimating the length of mixed oil. These intervals encompass the true length within a specified percentage  $\alpha$ , allowing workers to use the upper bound of the interval as a reference when excluding mixed oil. The upper bound only underestimate the mixed oil length by a probability of  $(1 - \alpha)/2$ , which can be much lower than 50%. Most importantly, in order to minimize the impact of the mixed oil segment on the quality of pure oil, on-site personnel typically allocate a certain margin during the batch cutting

operations for oil [29]. However, this margin is usually determined solely based on experience, with significant interference from human factors [30, 31]. The interval estimation method proposed in this article provides crucial data support for determining the cutting margin. This is of significant importance for improving the operational efficiency of the refined oil distribution network.

We propose confidence interval estimation of mixed oil lengths based on the pseudo samples generated by the diffusion model to measure the uncertainty in mixed oil length predictions. Furthermore, we propose to predict the mixed oil length using the mean of the generated pseudo samples. The main contributions of this paper can be summarized as:

- 1) Upon application to datasets collected from three operational pipelines, we use the diffusion model to provide interval estimation for the mixed oil length, and the effectiveness of our interval estimation is confirmed. The upper bound is suggested as a benchmark for the length of mixed oil when excluding it. It underestimates the mixed oil length with a probability of  $(1 - \alpha)/2$  theoretically, which can be much lower than 50%. In practical scenarios, when  $\alpha$  is set to 0.90, the upper limit of the interval underestimates the mixed oil length by only 6.8% and the average radius of the interval is approximately 300 meters.
- 2) Our proposed approach for predicting mixed oil length achieves a minimum of 14% improvement in accuracy when compared to commonly employed methods.

Given the presence of multiple notations in our paper, we provide detailed explanation of these symbols in Table 1 and Table 4.

## 2 Methodology

In this section, we begin by presenting deterministic methods for predicting the length of mixed oil. Subsequently, we introduce our proposed approach to establish confidence interval estimator for the length of mixed oil.

### 2.1 The deterministic methods

Austin et al. [7] formulated empirical equations for computing mixed oil based on actual pipeline data. Through extensive data analysis, they identified two distinct equations characterizing the relationship between mixed oil length and factors including transportation distance ( $L$ , in meters), pipeline inner diameter ( $d$ , in meters), and Reynolds numbers ( $Re$ ).



Table 1: The meanings of notations in the main paper.

Notations	Meanings
$\alpha$	The confidence level.
$L$	The transportation distance.
$d$	The inner diameter of the pipeline.
$Re$	The Reynolds number.
$Re_j$	The critical Reynolds number.
$C_0$	The initial mixed oil length.
$L_e$	The transportation distance in an equivalent pipeline corresponding to $C_0$ .
$L_c$	The calculated total transportation distance: $L + L_e$ .
$C_{AP}$	The calculated mixed oil length based on Austin-Palfrey equation.
$U(0, 10)$	The uniform distribution on $(0, 10)$
$N(0, 0.25)$	A normal distribution with a mean of 0 and a variance of 0.25
$Y$	A random variable, representing the mixed oil length.
$X$	A random variable, representing the pipeline feature.
$E(Y X)$	The conditional mean of $Y$ conditioned on $X$ .
$\{x_i, y_i\}_{i=1}^n$	The training dataset: $x_i$ is the pipeline feature, $y_i$ is the mixed oil length, and $n$ is the sample size.
$[y_i^{\alpha-low}, y_i^{\alpha-up}]$	The confidence interval used for bounding $y_i$ at a probability of $\alpha$ .
$P(y_i^{\alpha-low} \leq y_i \leq y_i^{\alpha-up}   x_i)$	The probability of $y_i$ falling in $[y_i^{\alpha-low}, y_i^{\alpha-up}]$ conditioned on $x_i$ .
$Y X$	The distribution of $Y$ conditioned on $X$ .
$N$	The number of pseudo samples.
$\{y_{i,l}\}_{l=1}^N$	The pseudo samples corresponding to $y_i$ .
$d_x$	The dimension of the pipeline feature.
$\hat{Y}$	An estimation of $E(Y X)$ .
$C_{AC}$	The true value of the mixed oil length.
$t \in \{0, 1, \dots, T\}$	The time steps in forward process and reverse process in the diffusion model.
$\{\beta_t\}_{t=1}^T$	The diffusion schedule, i.e., pre-set parameters in the diffusion model.

Specifically, the critical Reynolds number  $Re_j$  is defined as:

$$Re_j = 10000 \exp(2.72d^{0.5}). \quad (1)$$

Following [9], the initial mixed oil length  $C_0$  can be regarded as the result of batch transportation in an equivalent pipeline with length  $L_e$ :

$$L_e = \left( \frac{C_0 Re^{0.1}}{11.75d^{0.5}} \right)^2.$$

Then, the calculated total transportation distance is defined as

$$L_c = L + L_e.$$

Subsequently, the Austin-Palfrey equations apply in two scenarios. When Reynolds number  $Re$  is less than  $Re_j$ , the formula for calculating the mixed oil length is given by:

$$C_{AP} = 18384d^{0.5}L_c^{0.5}Re^{-0.9}\exp(2.18d^{0.5}). \quad (2)$$

When  $Re$  exceeds  $Re_j$ , the length of mixed oil can be significantly reduced [7, 9]. The calculation of mixed oil length is expressed as follows:

$$C_{AP} = 11.75d^{0.5}L_c^{0.5}Re^{-0.1}. \quad (3)$$

In our datasets, the Reynolds number  $Re$  spans from  $1.124 \times 10^5$  to  $8.819 \times 10^5$ . According to

(1),  $Re_j$  ranges from  $3.514 \times 10^4$  to  $6.856 \times 10^4$ . Therefore, the second Austin-Palfrey equation (3) is applied to our real pipeline datasets.

## 2.2 Confidence interval estimation

Numerous deterministic and machine learning methodologies [7, 16, 9, 17] have been proposed to estimate the length of mixed oil based on pipeline features. Nevertheless, these methods typically provide only a single point estimate, neglecting the inherent statistical variability. The point estimation for mixed oil length tends to exhibit a substantial probability, approximately 50%, of underestimating the actual length. To address this limitation, the statistical concept of confidence interval estimation can be used. Confidence interval estimation provides not just a point estimate but also a range, with a lower and upper bound, effectively addressing the uncertainty associated with point estimation.

Ignoring the definition of  $X$  and  $Y$  in Table 1 in this paragraph temporarily, let  $X \sim U(0, 10)$  and generate  $Y = \exp(\log(X) + \epsilon)$  with  $\epsilon \sim N(0, 0.25)$ . An intuitive comparison of point estimation and confidence interval estimation is provided in Figure 2. As depicted in the figure, the variance of  $Y$  increases with  $X$  due to the specific data generation mechanism, and the confidence interval can capture the uncertainty of  $Y$  as  $X$  varies. In contrast, point estimation only reflects the expected value of  $Y$  given  $X$ ,  $E(Y|X)$ , and cannot capture the uncertainty of  $Y$ .

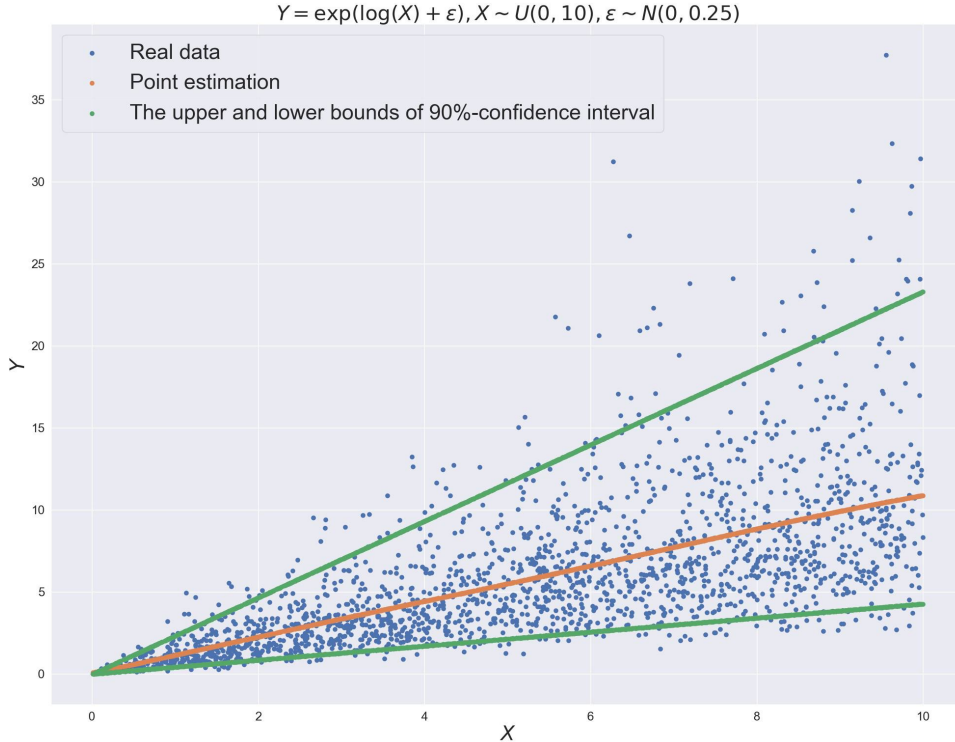


Figure 2: Comparison of point estimation and confidence interval estimation.

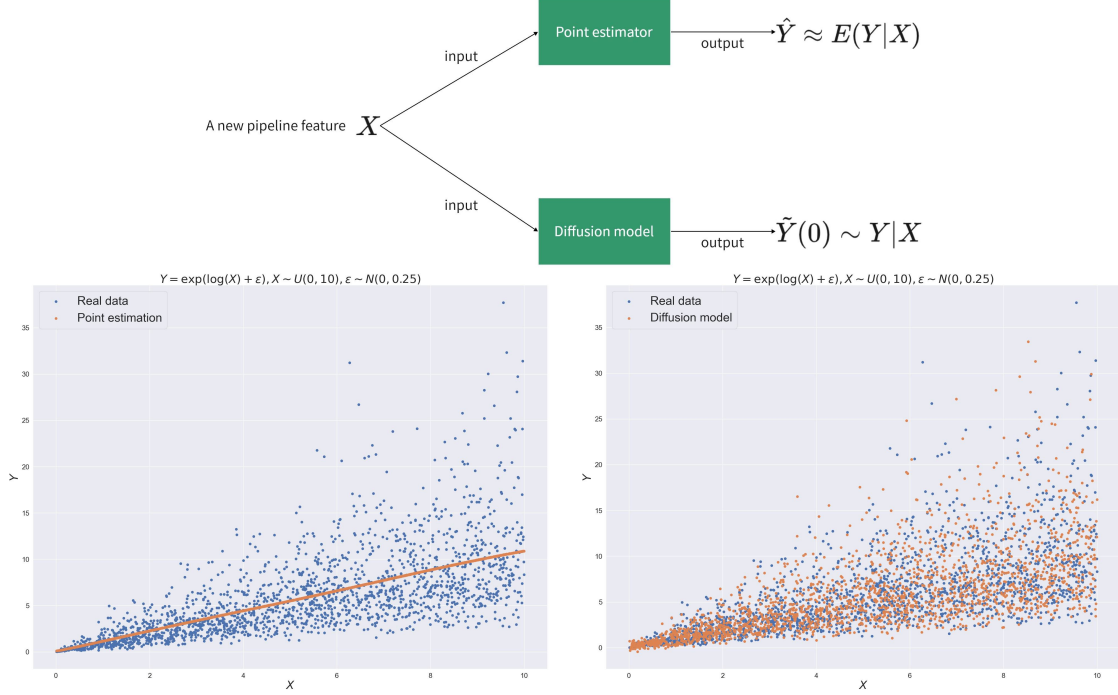


Figure 3: Comparison of the outputs of point estimator and diffusion model.

Next, we show the mathematical definition of confidence interval estimation. Considering a dataset encompassing  $n$  samples characterized by the observed pipeline features  $\{x_i\}_{i=1}^n$ , our objective, at a given confidence level  $\alpha$ , is to construct a confidence interval for the unknown mixed oil length  $y_i$ . This interval, denoted as  $[y_i^{\alpha-low}, y_i^{\alpha-up}]$ , is defined to satisfy

$$P(y_i^{\alpha-low} \leq y_i \leq y_i^{\alpha-up} | x_i) = \alpha,$$

and is established based on the corresponding pipeline features  $x_i$ , where  $i$  ranges from 1 to  $n$ . Assuming knowledge of the conditional distribution of  $Y|X$  with  $X$  representing the pipeline features and  $Y$  representing the mixed oil length, we can generate  $N$  pseudo samples denoted as  $\{y_{i,l}\}_{l=1}^N$  for the given  $x_i$ . Subsequently, from these  $N$  samples, we derive the upper  $(1 - \alpha)/2$  sample quantile and lower  $(1 - \alpha)/2$  sample quantile to obtain  $y_i^{\alpha-up}$  and  $y_i^{\alpha-low}$ , respectively. In practical applications, workers can then exclude  $y_i^{\alpha-up}$  meters of mixed oil, ensuring the exclusion of mixed oil by  $(1 + \alpha)/2$ . This probability can significantly exceed the probability (approximately 50%) of excluding mixed oil based on a single-point estimation. It's worth noting that the confidence level  $\alpha$  can typically be set to either 90% or 95%.

To conclude, the advantages of confidence interval estimation compared to point estimation lie in several aspects:

- 1) **Considering uncertainty:** Confidence interval estimation takes into account statistical error, thus better reflecting the true nature of the estimation results. In contrast, point estimation only provides a single estimator, inevitably lacking robustness and under-estimating

the mixed oil length.

- 2) **More reliable inference:** Confidence interval estimation provides a range that can be used to judge where the true value of mixed oil length. Such judgments are more reliable because they consider the uncertainty of the estimation, rather than relying solely on a point estimator.
- 3) **Greater adaptability:** Confidence interval estimation allows for the adjustment of the confidence level based on specific needs to fulfill various inferential requirements. This makes confidence interval estimation more flexible and adaptable.

## 2.3 Diffusion model

In Section 2.2, we assume that the conditional distribution of  $Y$  given  $X$  is known, and this serves as the foundation for constructing confidence interval estimates. Nonetheless, in reality, we do not have precise knowledge of this conditional distribution. So, we propose to learn this distribution using the conditional diffusion model [28]. Specifically, let  $\{x_i, y_i\}_{i=1}^n$  represent our training dataset, consisting of  $n$  samples used to train the diffusion model. In this context,  $x_i$  denotes the  $d_x$ -dimensional pipeline features, and  $y_i$  represents the corresponding mixed oil length. Utilizing Algorithm 1, the diffusion model has the capability to learn the conditional distribution  $Y$  given  $X$  from a given training set, and subsequently generate a predefined number of pseudo samples. Detailed descriptions of the diffusion model can be found in Appendix A.1.

Within the framework depicted in Figure 2, the difference between the point estimator and the diffusion model is illustrated in Figure 3. Specifically, the point estimator only learns the conditional mean  $E(Y|X)$  and outputs an estimator of  $E(Y|X)$ , whereas the diffusion model learns the conditional distribution of  $Y|X$  and outputs pseudo samples from  $Y|X$ .

## 2.4 Comparable distributions

In this article, we apply our method to a dataset obtained from the Supervisory Control and Data Acquisition (SCADA) system. This dataset comprises samples from three operational pipelines. For the training phase of our diffusion model, we use the 1781 samples from the first two pipelines. Subsequently, we assess the performance of our trained diffusion model using 528 samples from the third pipeline. To be specific, we utilize the pipeline features from the third pipeline as input to generate pseudo samples and establish confidence intervals for the mixed oil lengths.

Importantly, the diffusion model presented in Section 2.3 implicitly assume that the distribution

---

**Algorithm 1** Train the conditional diffusion model and generate pseudo samples

---

**Input:** Dataset  $\{x_i, y_i\}_{i=1}^n$ , max timestep  $T$ , diffusion schedule  $\{\beta_t\}_{t=1}^T$ , pre-trained model  $f_\phi(X)$ , an optimizer.

**Output:** A function to generate pseudo sample  $\tilde{Y}(0)$ .

```
1: Train the conditional diffusion model
2: Let  $\mathbf{X} = (x_1, x_2, \dots, x_n)^T$ ,  $\mathbf{Y}(0) = (y_1, y_2, \dots, y_n)^T$ 
3: Initialize a neural network  $nn_\theta$ ,  $\theta$  represents the parameters of  $nn_\theta$ 
4: While not converge:
5:   Randomly draw  $t$  from  $\{1, 2, \dots, T\}$ 
6:   Let  $\alpha_t = 1 - \beta_t$ ,  $\bar{\alpha}_t = \prod_{s=1}^t \alpha_s$ 
7:   Draw  $\epsilon_{0 \rightarrow t} \sim N(0, I_{n \times n})$ 
8:   Let  $\mathbf{Y}(t) = \sqrt{\bar{\alpha}_t} \mathbf{Y}(0) + (1 - \sqrt{\bar{\alpha}_t}) f_\phi(\mathbf{X}) + \sqrt{1 - \bar{\alpha}_t} \epsilon_{0 \rightarrow t}$ 
9:   Compute  $\mathbf{L}_\theta = \|\epsilon_{0 \rightarrow t} - nn_\theta(\mathbf{X}, \mathbf{Y}(t), f_\phi(\mathbf{X}), t)\|^2$ 
10:  Take optimization step on  $\mathbf{L}_\theta$  and update  $\theta$  via the optimizer
11: end While

12: Function  $G(X)$ :  $\triangleright$  Function to generate pseudo samples based on each new
    pipeline feature  $X$ 
13:  Draw  $\tilde{Y}(T) \sim N(f_\phi(X), 1)$ 
14:  For  $t$  from  $T$  to 1:
15:    Let  $\hat{Y}^t(0) = \frac{1}{\sqrt{\bar{\alpha}_t}} \left[ \tilde{Y}(t) - (1 - \sqrt{\bar{\alpha}_t}) f_\phi(X) - \sqrt{1 - \bar{\alpha}_t} nn_\theta(X, \tilde{Y}(t), f_\phi(X), t) \right]$ 
16:    Let  $\tilde{\mu}(\hat{Y}^t(0), \tilde{Y}(t), X) = \frac{\beta_t \sqrt{\bar{\alpha}_{t-1}}}{1 - \bar{\alpha}_t} \hat{Y}^t(0) + \frac{(1 - \bar{\alpha}_{t-1}) \sqrt{\bar{\alpha}_t}}{1 - \bar{\alpha}_t} \tilde{Y}(t) +$ 
         $\left( 1 + \frac{(\sqrt{\bar{\alpha}_t} - 1)(\sqrt{\bar{\alpha}_t} + \sqrt{\bar{\alpha}_{t-1}})}{1 - \bar{\alpha}_t} \right) f_\phi(X)$ 
17:    Draw  $\epsilon_{t \rightarrow (t-1)}$  from  $N(0, 1)$ 
18:     $\tilde{Y}(t-1) = \tilde{\mu}(\hat{Y}^t(0), \tilde{Y}(t), X) + \sqrt{\tilde{\beta}_t} \epsilon_{t \rightarrow (t-1)}$   $\triangleright$  The definition of  $\tilde{\beta}_t$  can be found
        in (9)
19:  end For
20:  Return  $\tilde{Y}(0)$ 
21: end Function
```

---

of the mixed oil length for the first two pipelines (training dataset) matches or closely resembles the distribution for the third pipeline (testing dataset). We use  $C_{AC}$  to represent the true value of the mixed oil length. As depicted in the left panel of Figure 4, significant disparities in the distribution of  $C_{AC}$  exist between the first two pipelines and the third pipeline [32, 16]. This difference presents a considerable challenge to the generalization capability of our proposed diffusion model.

We obtain a preliminary estimation of the mixed oil length  $C_{AP}$  using the Austin-Palfrey formula mentioned in Section 2.1. Subsequently, we calculate the difference between the true value  $C_{AC}$  and  $C_{AP}$ , i.e.,  $C_{AC} - C_{AP}$ . As shown in the right panel of Figure 4, the distribution of  $C_{AC} - C_{AP}$  in the first two pipelines is comparable to that in the third pipeline [16]. Therefore, in Section

2.3, given the pipeline feature, instead of learning the distribution of the mixed oil length, we propose to learn the distribution of  $C_{AC} - C_{AP}$ . For a pipeline feature from the third pipeline, once we generate  $N$  pseudo samples of  $C_{AC} - C_{AP}$  using the diffusion model, we can acquire  $N$  pseudo samples of the mixed oil length by adding  $C_{AP}$  to each sample within the pseudo samples of  $C_{AC} - C_{AP}$ . The flowchart depicting our proposed method can be found in Figure 5.

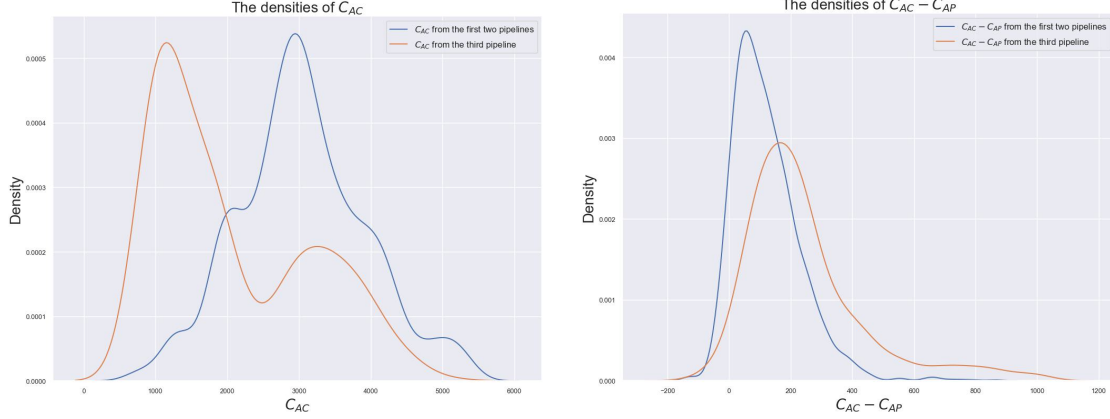


Figure 4: Left panel: estimated density functions of  $C_{AC}$  in the training and testing sets. Right panel: estimated density functions of  $C_{AC} - C_{AP}$  in the training and testing sets.

### 3 Case Studies

#### 3.1 Data processing

In this section, we apply our approach to a dataset gathered from the SCADA system. Given the inevitable presence of measurement errors, immeasurable noise, or inaccuracies in recording, outliers are present in the dataset. Following the approach in [9], we computed the relative error between  $C_{AP}$  and the actual value  $C_{AC}$ . If the relative error of a specific sample exceeds 20%, it is designated as an outlier and subsequently removed from the dataset. Consequently, 26 samples from the first two pipelines were excluded.

#### 3.2 Feature selection

The features from the collected on-site mixed oil data include transmission distance  $L$ , diameter  $d$ , initial mixed oil length  $C_0$ , and Reynolds number  $Re$ . The second Austin-Palfrey equation (3) is applied to our real pipeline datasets to calculate  $C_{AP}$  as mentioned in subsection 2.1. We have conducted experiments to demonstrate that the calculated value  $C_{AP}$  is the most

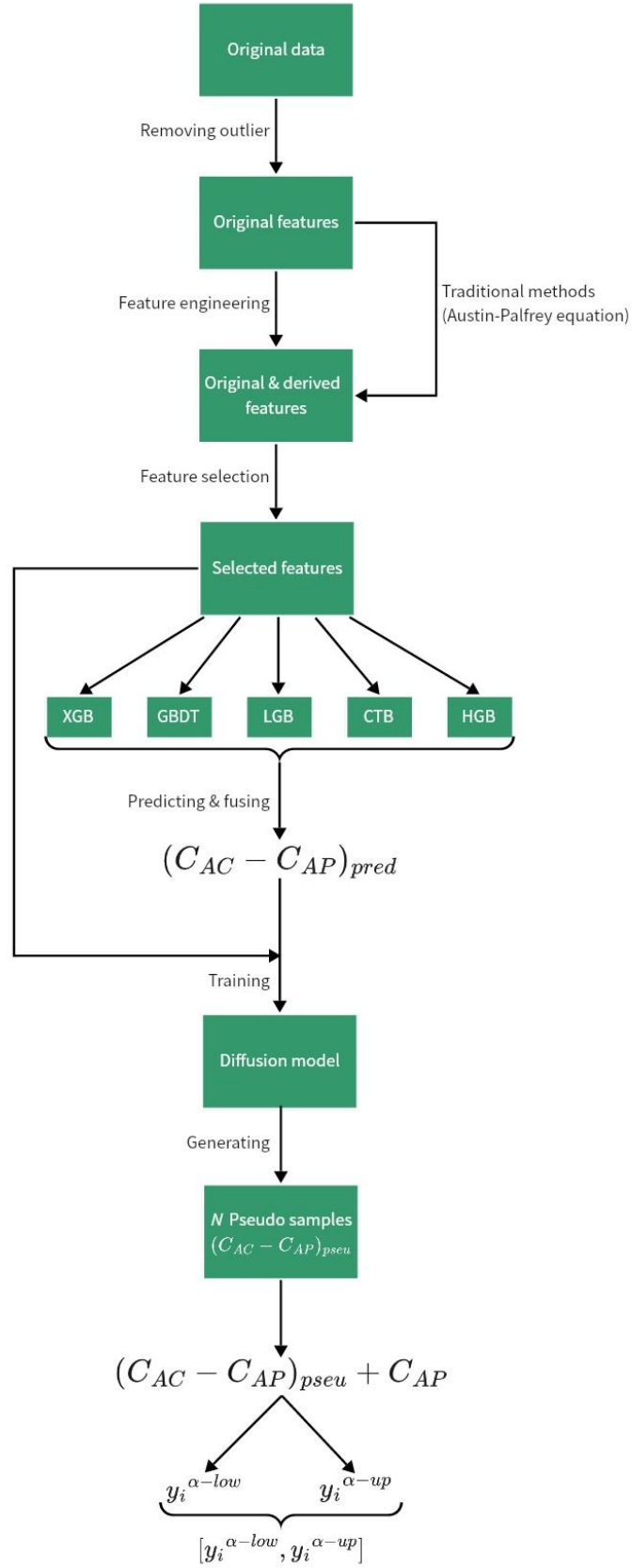


Figure 5: The flow chart of our proposed method.

important feature. Motivated by [9], the following two more features are as alternatives:

$$d' = d^{0.5}, \quad Re' = Re^{-0.1}.$$

Based on the variable importance outputted by XGBoost [33], we choose the initial oil mixture  $C_0$ , the formula-calculated value  $C_{AP}$ , and the transformed features  $d'$  and  $Re'$  as the input pipeline features for our proposed diffusion model.

### 3.3 Pre-trained model and the diffusion schedule

Five ensemble tree models, specifically XGBoost [33], GBDT [15], LGB [34], CTB [35], and HGB [36], are utilized to capture the relationship between the selected pipeline features  $X$  and  $C_{AC} - C_{AP}$  individually. The pretrained model is obtained by combining the predictions from these five models. To be specific, the prediction of the pretrained model is the average of the results obtained from these five models. Within the diffusion model, the diffusion schedule  $\{\beta_t\}_{t=1}^T$  is configured to increase linearly from  $\beta_1 = 10^{-5}$  to  $\beta_T = 2 \cdot 10^{-3}$ , with the maximum timestep  $T$  set to 1000.

### 3.4 Interval estimation of mixed oil length

We randomly select 70% samples of the first two pipelines as the training set and 30% as the validation set. Samples from the training set are used to train our models and samples from the validation set are used to tune parameters. The samples from the third pipeline are taken as the test set. For each feature  $X$  from the test set, we draw  $N = 200$  pseudo samples from the diffusion model. The generated confidence interval estimations are shown in Figure 6 with confidence levels 90% and 95%.

Besides our proposed method, we also consider the Austin-Palfrey equation, the Gaussian mixture regression [18], Chen’s method [9], and Yuan’s method [16]. From Table 2, we can find that the Austin-Palfrey formula is highly likely to significantly underestimate the length of the oil mix, with a probability exceeding 98%, while the approaches in [18], [9] and [16] exhibit probabilities of 88.8%, 35.7% and 47.4%, respectively. Our interval estimation method effectively provides a confidence upper limit for the mixed oil length at the confidence level  $\alpha$ . It is worth noting that, at the expense of excluding approximately 300 more meters of oil, the proposed confidence upper limit underestimates the length of mixed oil with probabilities of 6.8% and 4.9% when  $\alpha$  is set to 90% and 95%, respectively.

Therefore, pipeline companies have the flexibility to determine the confidence level  $\alpha$  based on



their specific requirements and, accordingly, can exclude the mixed oil at the upper limit.

Moreover, we use the mean of the pseudo samples generated by the diffusion model as an estimator for mixed oil length. We then compare the prediction accuracy among different methods. Specifically, following [9] and [16], we employ RMSE,  $R^2$ , and MAE to assess the performance:

$$\text{RMSE} = \sqrt{\frac{1}{n} \sum_{i=1}^n (y_i - \hat{y}_i)^2}, \quad (4)$$

$$R^2 = 1 - \frac{\sum_{i=1}^n (y_i - \hat{y}_i)^2}{\sum_{i=1}^n (y_i - \bar{y}_i)^2},$$

$$\text{MAE} = \frac{1}{n} \sum_{i=1}^n |y_i - \hat{y}_i|,$$

where  $y_i$ ,  $\hat{y}_i$ , and  $\bar{y}_i$  represent the actual value, predicted value, and sample mean of the length of the mixed oil in the test set. A large  $R^2$  is preferred, while small RMSE and MAE are desired. The results are shown in Table 3. It is observed that our proposed method outperforms the other four methods in terms of the three criteria. For example, in comparison to Yuan’s method, which serves as the best baseline, our approach achieves a reduction in MAE by approximately 14%. Furthermore, Figure 7 compares the scatter plots of predicted values from various methods with the true values for the third pipeline. The closer the scatter plot of predicted values is to that of the true  $C_{AC}$ , the better the model fitting. It is evident that our proposed method outperforms the other four methods in this comparison.

Table 2: The probability of underestimating the length of mixed oil using different methods.

Models	Probability
Austin-Palfrey equation	98.3%
Gaussian mixture regression	88.8%
Chen’s method	35.7%
Yuan’s method	47.4%
Upper limit ( $\alpha = 0.90$ )	6.8%
Upper limit ( $\alpha = 0.95$ )	<b>4.9%</b>

Table 3: The RMSEs,  $R^2$ s and MAEs for predictions of mixed oil length using various methods.

Models	<i>RMSE</i>	$R^2$	<i>MAE</i>
Austin-Palfrey equation	311.065	0.916	245.037
Gaussian mixture regression	244.938	0.948	177.783
Chen’s method	207.007	0.963	160.773
Yuan’s method	185.849	0.970	144.543
Our method	<b>171.913</b>	<b>0.974</b>	<b>123.991</b>

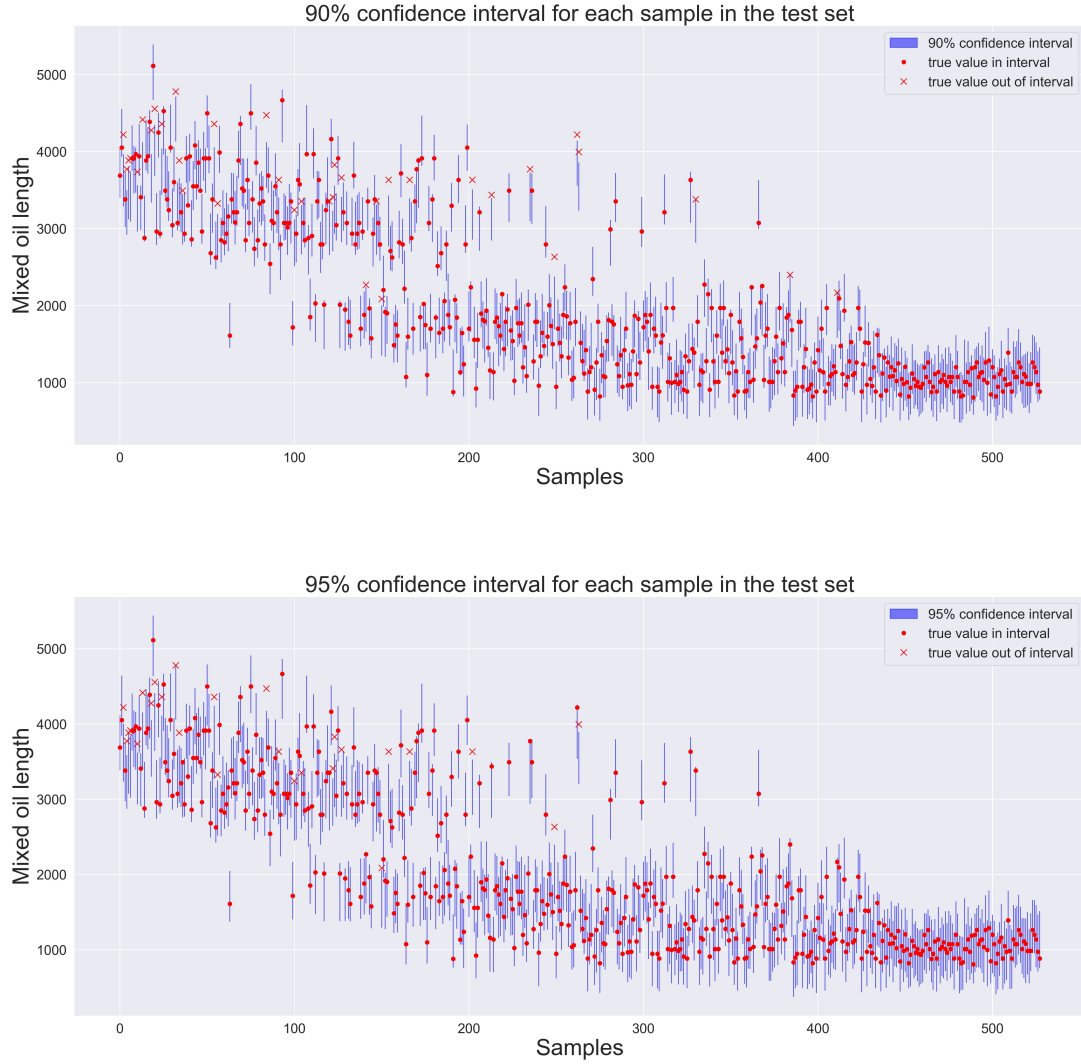


Figure 6: Interval estimations of mixed oil lengths for the third pipeline with confidence levels of 0.9 and 0.95. At a confidence level of 90%, there are 36 samples falling outside the intervals, achieving a coverage rate of 93.2%, with an average radius of 317.0 for the intervals. At a 95% confidence level, there exist 26 samples outside the intervals, exhibiting a coverage rate of 95.1%, with the intervals having an average radius of 378.5.

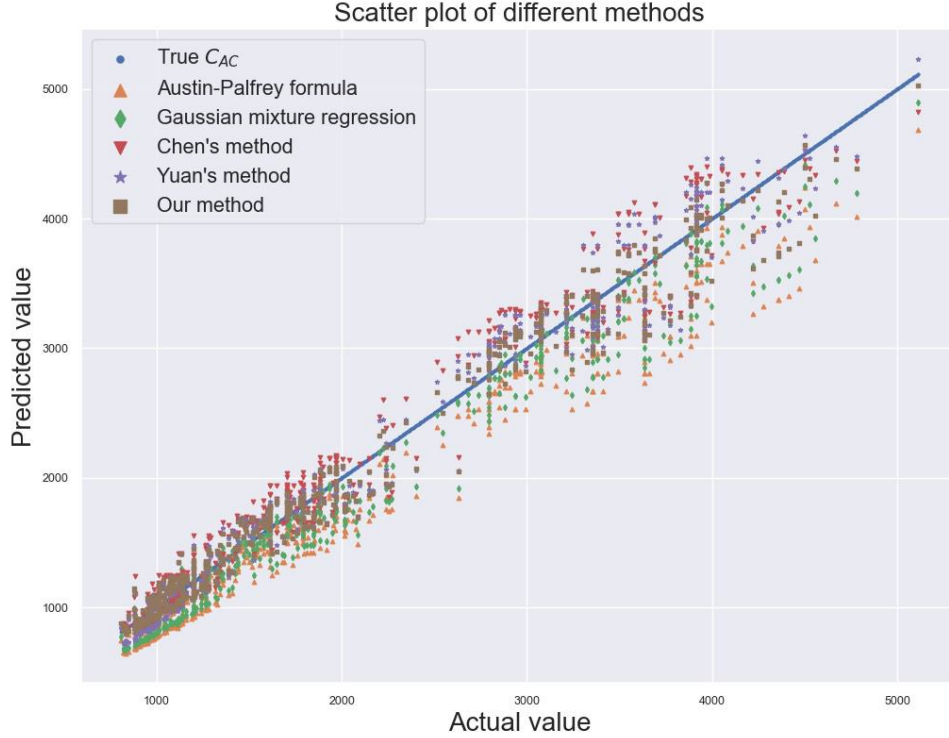


Figure 7: Scatter plot comparisons among various models for the third pipelines.

## 4 Conclusion

Mixed oil is inevitably formed during the batch transportation in product pipelines. The presence of mixed oil can result in a deterioration of the quality of oil products, impacting factors such as octane number, flash point, and final boiling point. This can lead to the refined products being of substandard quality [37]. For example, the South China Multi-Product Pipeline Network Company expends millions of CNY annually on the treatment of mixed oil [8]. The utilization of off-specification oil products in machinery can result in equipment malfunctions, potentially compromising the operational reliability of gasoline engines and aviation equipment [38]. Therefore, it is of utmost importance to prevent the ingress of mixed oil into the refined oil products.

In this article, we propose the utilization of the conditional diffusion model to establish a confidence interval for the mixed oil length. Our proposed upper limit of the interval ensures a high probability of excluding mixed oil, addressing the limitations of previous methods that solely provide point estimations. The conventional approaches often result in underestimation of the mixed oil length, contributing to significant quality loss with an extremely high probability. Therefore, the upper limit of the constructed confidence interval can serve as a reference for pipeline companies to exclude mixed oil. This approach can help in reducing unnecessary costs while maintaining high oil product quality. Additionally, using the mean of the pseudo samples generated by the diffusion model as a point estimator of the mixed oil length proves to be more

effective than previous commonly used methods.

To mitigate the influence of the mixed oil segment on the purity of the oil, personnel on-site commonly set aside a specific buffer during oil batch cutting operations [29]. However, this buffer is often decided solely through experience, with notable interference from human factors [30, 31]. The interval estimation method proposed in this article offers essential data support in establishing the cutting buffer. This is notably crucial for enhancing the operational efficiency of the refined oil distribution network.

## Credit author statement

Yanfeng Yang: Conceptualization, Methodology, Writing - Original Draft. Lihong Zhang: Writing - Original Draft. Ziqi Chen: Supervision, Writing - Original draft, Writing - Review & Editing. Miaomiao Yu: Validation. Lei Chen: Data curation.

## Declaration of competing interest

To the best of our knowledge and belief, this manuscript has neither been published in whole nor in part, nor is it currently under consideration for publication elsewhere. We declare that we have no known competing financial interests or personal relationships that could be perceived to influence the work reported in this paper.

## Data availability

The data that has been used is confidential.

## Acknowledgement

Dr. Ziqi Chen's work was partially supported by the National Key R&D Program of China (2021YFA1000100 and 2021YFA1000101), National Natural Science Foundation of China (NSFC) (12271167, 11871477 and 72331005), and Natural Science Foundation of Shanghai (21ZR1418800).

## References

- [1] Cheryl J Trench. How pipelines make the oil market work—their networks, operation and regulation, 2001. <https://www.iatp.org/documents/how-pipelines-make-the-oil-market-work-their-networks-operation-and-regulation/> (accessed 04 June 2024).
- [2] Chao Chen, Changjun Li, Genserik Reniers, and Fuqiang Yang. Safety and security of oil and gas pipeline transportation: A systematic analysis of research trends and future needs using wos. *Journal of Cleaner Production*, 279:123583, 2021.
- [3] Liqiao Huang, Qi Liao, Jinyue Yan, Yongtu Liang, and Haoran Zhang. Carbon footprint of oil products pipeline transportation. *Science of the Total Environment*, 783:146906, 2021.
- [4] SA MirHassani, M Abbasi, and S Moradi. Operational scheduling of refined product pipeline with dual purpose depots. *Applied Mathematical Modelling*, 37(8):5723–5742, 2013.
- [5] SA MirHassani and H Fani Jahromi. Scheduling multi-product tree-structure pipelines. *Computers & chemical engineering*, 35(1):165–176, 2011.
- [6] Wassila Abdellaoui, Mehdi Souier, M’hammed Sahnoun, and Fouad Ben Abdelaziz. Multi-period optimal schedule of a multi-product pipeline: A case study in algeria. *Computers & Industrial Engineering*, 159:107483, 2021.
- [7] JE Austin and JR Palfrey. Mixing of miscible but dissimilar liquids in serial flow in a pipeline. *Proceedings of the Institution of Mechanical Engineers*, 178(1):377–389, 1963.
- [8] Jian Du, Jianqin Zheng, Yongtu Liang, Yuheng Xia, Bohong Wang, Qi Shao, Qi Liao, Renfu Tu, Bin Xu, and Ning Xu. Deeppipe: An intelligent framework for predicting mixed oil concentration in multi-product pipeline. *Energy*, 282:128810, 2023.
- [9] Lei Chen, Ziyun Yuan, JianXin Xu, Jingyang Gao, Yuhan Zhang, and Gang Liu. A novel predictive model of mixed oil length of products pipeline driven by traditional model and data. *Journal of Petroleum Science and Engineering*, 205:108787, 2021.
- [10] Anirudh R Patrachari and Arland H Johannes. A conceptual framework to model interfacial contamination in multiproduct petroleum pipelines. *International journal of heat and mass transfer*, 55(17-18):4613–4620, 2012.
- [11] Yansong Li, Dong Han, Baoying Wang, and Jianfei Sun. An industrial scale simulation method for predicting the contamination evolution in long-distance multiproduct pipelines. *Journal of Pipeline Systems Engineering and Practice*, 14(1):04022054, 2023.
- [12] Yi Wang, Baoying Wang, Yang Liu, and Yongtu Liang. Study on asymmetry concentration of mixed oil in products pipeline. *Energies*, 13(23):6398, 2020.

- [13] Vali Hamidi, Ebrahim Hajidavalloo, and Morteza Behbehani-Nejad. Numerical simulation of mixing between sequential fluids in a pipeline considering real conditions. *Chemical Engineering & Technology*, 46(4):644–653, 2023.
- [14] Xu Li, Wenxue Han, Weiming Shao, Lei Chen, and Dongya Zhao. Data-driven predictive model for mixed oil length prediction in long-distance transportation pipeline. *in: Proceedings of the IEEE 10th Data Driven Control and Learning Systems Conference (DDCLS)*, pages 1486–1491, 2021.
- [15] Jerome H Friedman. Greedy function approximation: a gradient boosting machine. *Annals of statistics*, pages 1189–1232, 2001.
- [16] Ziyun Yuan, Lei Chen, Weiming Shao, Zhiheng Zuo, Wan Zhang, and Gang Liu. A robust hybrid predictive model of mixed oil length with deep integration of mechanism and data. *Journal of Pipeline Science and Engineering*, 1(4):459–467, 2021.
- [17] Ziyun Yuan, Lei Chen, Gang Liu, Weiming Shao, Yuhan Zhang, and Yunxiu Ma. Physics-informed student’s t mixture regression model applied to predict mixed oil length. *Journal of Pipeline Science and Engineering*, 3(1):100105, 2023.
- [18] Ziyun Yuan, Lei Chen, Gang Liu, and Yuhan Zhang. Knowledge-informed variational bayesian gaussian mixture regression model for predicting mixed oil length. *Energy*, 285:129248, 2023.
- [19] Jonathan Ho, Ajay Jain, and Pieter Abbeel. Denoising diffusion probabilistic models. *in: Advances in neural information processing systems*, 33:6840–6851, 2020.
- [20] Prafulla Dhariwal and Alexander Nichol. Diffusion models beat gans on image synthesis. *in: Advances in neural information processing systems*, 34:8780–8794, 2021.
- [21] Xiang Li, John Thickstun, Ishaan Gulrajani, Percy S Liang, and Tatsunori B Hashimoto. Diffusion-lm improves controllable text generation. *in: Advances in Neural Information Processing Systems*, 35:4328–4343, 2022.
- [22] Robin Rombach, Andreas Blattmann, Dominik Lorenz, Patrick Esser, and Björn Ommer. High-resolution image synthesis with latent diffusion models. In *Proceedings of the IEEE/CVF conference on computer vision and pattern recognition*, pages 10684–10695, 2022.
- [23] Chitwan Saharia, William Chan, Saurabh Saxena, Lala Li, Jay Whang, Emily L Denton, Kamyar Ghasemipour, Raphael Gontijo Lopes, Burcu Karagol Ayan, Tim Salimans, et al. Photorealistic text-to-image diffusion models with deep language understanding. *in: Advances in Neural Information Processing Systems*, 35:36479–36494, 2022.
- [24] Kashif Rasul, Calvin Seward, Ingmar Schuster, and Roland Vollgraf. Autoregressive denoising diffusion models for multivariate probabilistic time series forecasting. *in: International Conference on Machine Learning*, pages 8857–8868, 2021.

- [25] Jiaming Song, Chenlin Meng, and Stefano Ermon. Denoising diffusion implicit models. *arXiv preprint arXiv:2010.02502*, 2020.
- [26] Fan Bao, Chongxuan Li, Jun Zhu, and Bo Zhang. Analytic-dpm: an analytic estimate of the optimal reverse variance in diffusion probabilistic models. *arXiv preprint arXiv:2201.06503*, 2022.
- [27] Alexander Quinn Nichol and Prafulla Dhariwal. Improved denoising diffusion probabilistic models. *in: International Conference on Machine Learning*, pages 8162–8171, 2021.
- [28] Xizewen Han, Huangjie Zheng, and Mingyuan Zhou. Card: Classification and regression diffusion models. *in: Advances in Neural Information Processing Systems*, 35:18100–18115, 2022.
- [29] Xue Li, Xiaolin Wang, and Wentao Xiao. Two-section cutting method of contamination in products pipeline by dynamic volume fraction judgment. *Oil & Gas Storage and Transportation*, 36(10):1149–1153, 2017.
- [30] Timothy R Harbert. Automation improvements in batch cutting process: The last profit center for pipelines. In *International Pipeline Conference*, volume 48579, pages 623–628, 2008.
- [31] Jianqin Zheng, Jian Du, Yongtu Liang, Bohong Wang, Miao Li, Qi Liao, and Ning Xu. Deeppipe: A hybrid intelligent framework for real-time batch tracking of multi-product pipelines. *Chemical Engineering Research and Design*, 191:236–248, 2023.
- [32] Douglas A Reynolds. Gaussian mixture models. *Encyclopedia of biometrics*, 741:659–663, 2009.
- [33] Tianqi Chen and Carlos Guestrin. Xgboost: A scalable tree boosting system. *in: Proceedings of the 22nd acm sigkdd international conference on knowledge discovery and data mining*, pages 785–794, 2016.
- [34] Guolin Ke, Qi Meng, Thomas Finley, Taifeng Wang, Wei Chen, Weidong Ma, Qiwei Ye, and Tie-Yan Liu. Lightgbm: A highly efficient gradient boosting decision tree. *in: Advances in neural information processing systems*, 30:3149–3157, 2017.
- [35] Liudmila Prokhorenkova, Gleb Gusev, Aleksandr Vorobev, Anna Veronika Dorogush, and Andrey Gulin. Catboost: unbiased boosting with categorical features. *in: Advances in neural information processing systems*, 31:6639–6649, 2018.
- [36] Hanyuan Hang, Tao Huang, Yuchao Cai, Hanfang Yang, and Zhouchen Lin. Gradient boosted binary histogram ensemble for large-scale regression. *arXiv preprint arXiv:2106.01986*, 2021.

- [37] Jian Du, Jianqin Zheng, Yongtu Liang, Ning Xu, Jiří Jaromír Klemesš, Bohong Wang, Qi Liao, Petar Sabev Varbanov, Khurram Shahzad, and Arshid Mahmood Ali. Deeppipe: A two-stage physics-informed neural network for predicting mixed oil concentration distribution. *Energy*, 276:127452, 2023.
- [38] Rustam Sunagatullin, Fedor Timofeev, Andrey Kuznetsov, and Yulia Oludina. Relevant issues on quality evaluation of petroleum pipeline preparation for oil product transportation. *Oil & Gas Science and Technology–Revue d’IFP Energies nouvelles*, 74:44, 2019.
- [39] Diederik P Kingma and Jimmy Ba. Adam: A method for stochastic optimization. *arXiv preprint arXiv:1412.6980*, 2014.
- [40] Lingxin Hao and Daniel Q Naiman. *Quantile regression*. Number 149. Sage, Thousand Oaks, California, 1st edition, 2007.
- [41] Nicolai Meinshausen. Quantile regression forests. *Journal of Machine Learning Research*, 7(35):983–999, 2006.
- [42] Yaniv Romano, Evan Patterson, and Emmanuel Candes. Conformalized quantile regression. *in: Advances in Neural Information Processing Systems*, 32:3538–3548, 2019.

## A Appendix

This appendix provides supplementary information to complement the main paper, including the detailed descriptions of the conditional diffusion model [28] and a comparative analysis with alternative confidence interval estimation methods.

### A.1 Diffusion model

In practical scenarios, the conditional distribution of  $Y|X$  is unknown. We propose to learn this distribution using the diffusion model. Specifically, let  $\{x_i, y_i\}_{i=1}^n$  represent our training dataset, consisting of  $n$  samples used to train the diffusion model. In this context,  $x_i$  denotes the  $d_x$ -dimensional pipeline features, and  $y_i$  represents the corresponding mixed oil length. The conventional diffusion model is primarily designed for learning unconditional distributions. We aim to learn the conditional distribution of  $Y|X$ . In our approach, we integrate a pre-trained model  $f_\phi(X)$  into the original diffusion model [28], enabling it to capture the conditional distribution of the original data given  $f_\phi(X)$  (i.e.,  $Y|f_\phi(X)$ ). When  $f_\phi(X)$  performs well,  $Y|f_\phi(X)$  closely approximates  $Y|X$ . Utilizing this conditional distribution  $Y|f_\phi(X)$ , we input



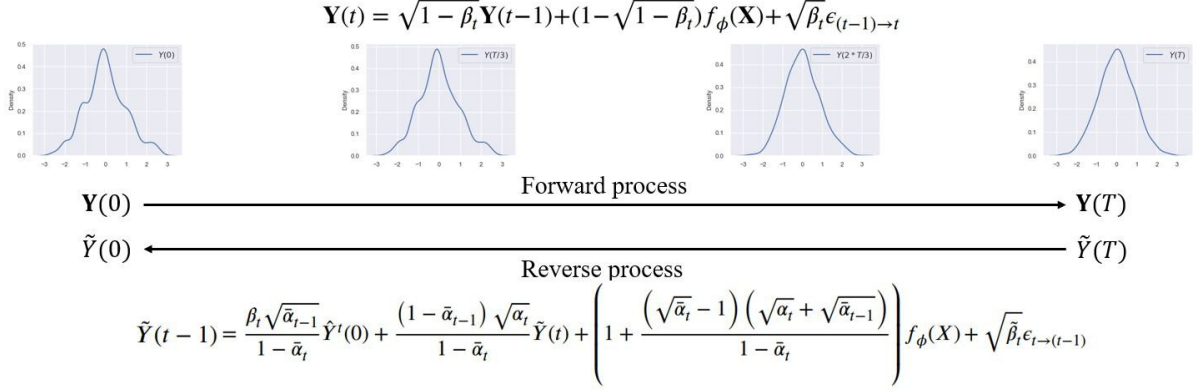


Figure 8: The diagram of diffusion model.

Table 4: The meanings of notations in the Appendix.

Notations	Meanings
$\alpha_t$	$\alpha_t = 1 - \beta_t$ .
$\bar{\alpha}_t$	$\bar{\alpha}_t = \prod_{s=1}^t \alpha_s$ .
$f_\phi(X)$	A pre-trained model, predicting $E(Y X)$ .
$\mathbf{X}$	$\mathbf{X} = (x_1, x_2, \dots, x_n)^T$ .
$\mathbf{Y}(0)$	$\mathbf{Y}(0) = (y_1, y_2, \dots, y_n)^T$ .
$\epsilon_{i \rightarrow j}$	A standard $n$ -dimensional Gaussian variable, used to transform $\mathbf{Y}(i)$ to $\mathbf{Y}(j)$ .
$I_{n \times n}$	The $n$ -dimensional identity matrix.
$N(0, I_{n \times n})$	A standard $n$ -dimensional normal distribution.
$\mathbf{Y}(t)$	The latent variables in the forward process of the diffusion model.
$\mathbf{L}_\theta$	The loss function of the diffusion model.
$nn_\theta$	A deep neural network, $\theta$ represents the parameters of the deep neural network.
$\tilde{Y}(t)$	The latent variables in the reverse process of the diffusion model.
$\hat{Y}^t(0)$	An estimation of $Y(0)$ based on $Y(t)$ .
$\tilde{\mu}(Y(0), \tilde{Y}(t), X)$	The mean in (8).
$\tilde{\beta}_t$	The variance in (8).

new pipeline features  $X$  into  $Y|f_\phi(X)$  to generate pseudo samples. These pseudo samples are used to construct the confidence interval estimation as described in Section 2.2.

Let  $t \in \{0, 1, \dots, T\}$  be the time steps in both the forward and reverse processes in the diffusion model. Consider the pre-trained model  $f_\phi(X)$ , which is used to predict  $Y$  and will be introduced in Section 3.3. Let  $\{\beta_t\}_{t=1}^T$  with  $\beta_t \in (0, 1)$  be the diffusion schedule. Define  $\alpha_t := 1 - \beta_t$  and  $\bar{\alpha}_t := \prod_{s=1}^t \alpha_s$ . Let  $\mathbf{Y}(t)$ , for  $t = 1, \dots, T$ , represent the latent variables in the forward processes. Define  $\mathbf{X} := (x_1, x_2, \dots, x_n)^T$  and  $\mathbf{Y}(0) := (y_1, y_2, \dots, y_n)^T$ . For  $t = 1, \dots, T$ , define

$$\mathbf{Y}(t) = \sqrt{1 - \beta_t} \mathbf{Y}(t-1) + \left(1 - \sqrt{1 - \beta_t}\right) f_\phi(\mathbf{X}) + \sqrt{\beta_t} \epsilon_{(t-1) \rightarrow t},$$

where  $\epsilon_{(t-1) \rightarrow t} \sim N(0, I_{n \times n})$  with  $I_{n \times n}$  being the  $n$ -dimensional identity matrix. Thus, we have

$$\mathbf{Y}(t) | \mathbf{Y}(t-1), f_\phi(\mathbf{X}) \sim N(\sqrt{\alpha_t} \mathbf{Y}(t-1) + (1 - \sqrt{\alpha_t}) f_\phi(\mathbf{X}), \beta_t I). \quad (5)$$

Then, we obtain

$$\begin{aligned} \mathbf{Y}(t) &= \sqrt{1 - \beta_t} \left[ \sqrt{1 - \beta_{t-1}} \mathbf{Y}(t-2) \right. \\ &\quad \left. + \left(1 - \sqrt{1 - \beta_{t-1}}\right) f_\phi(\mathbf{X}) + \sqrt{\beta_{t-1}} \epsilon_{(t-2) \rightarrow (t-1)} \right] \\ &\quad + \left(1 - \sqrt{1 - \beta_t}\right) f_\phi(\mathbf{X}) + \sqrt{\beta_t} \epsilon_{(t-1) \rightarrow t} \\ &= \sqrt{\alpha_t \alpha_{t-1}} \mathbf{Y}(t-2) + (1 - \sqrt{\alpha_t \alpha_{t-1}}) f_\phi(\mathbf{X}) \\ &\quad + \sqrt{1 - \alpha_t \alpha_{t-1}} \epsilon_{(t-2) \rightarrow t}, \end{aligned}$$

where  $\epsilon_{(t-2) \rightarrow t} \sim N(0, I_{n \times n})$ . Similarly, we represent  $\mathbf{Y}(t)$  as a function of  $\mathbf{Y}(0)$ :

$$\mathbf{Y}(t) = \sqrt{\bar{\alpha}_t} \mathbf{Y}(0) + (1 - \sqrt{\bar{\alpha}_t}) f_\phi(\mathbf{X}) + \sqrt{1 - \bar{\alpha}_t} \epsilon_{0 \rightarrow t}, \quad (6)$$

where  $\epsilon_{0 \rightarrow t} \sim N(0, I_{n \times n})$ . Thus, the distribution of  $\mathbf{Y}(t)$  given  $\mathbf{Y}(0)$  and  $f_\phi(\mathbf{X})$  can be written as:

$$\begin{aligned} \mathbf{Y}(t) | \mathbf{Y}(0), f_\phi(\mathbf{X}) &\sim N(\sqrt{\bar{\alpha}_t} \mathbf{Y}(0) + (1 - \sqrt{\bar{\alpha}_t}) f_\phi(\mathbf{X}), \\ &\quad (1 - \bar{\alpha}_t) I_{n \times n}). \end{aligned} \quad (7)$$

When  $T \rightarrow \infty$ ,  $\bar{\alpha}_T \rightarrow 0$ . So,  $\mathbf{Y}(T) | \mathbf{Y}(0), f_\phi(\mathbf{X})$  converges to  $N(f_\phi(\mathbf{X}), I_{n \times n})$ .

Next, we describe the procedure for generating pseudo samples of  $Y|X$  based on a given new pipeline feature  $X \in \mathbb{R}^{1 \times d_x}$ . In particular, this is achieved through the reverse process of the previously mentioned forward process. Initially, we generate noise  $\tilde{Y}(T)$  from  $N(f_\phi(X), 1)$ . Subsequently, we aim to transform  $\tilde{Y}(T)$  into high-quality pseudo samples of  $Y|X$ , denoted as  $\tilde{Y}(0)$ .

Let  $\tilde{Y}(t), t = T-1, \dots, 1$  be the latent variables in the reverse process. According to Bayes'

theorem, (5), (7) and the Markov property of the forward process, we derive the distribution of  $\tilde{Y}(t-1)$  conditional on  $(\tilde{Y}(t), Y(0), f_\phi(X))$ :

$$\tilde{Y}(t-1)|\tilde{Y}(t), Y(0), f_\phi(X) \sim N\left(\tilde{\mu}\left(Y(0), \tilde{Y}(t), X\right), \tilde{\beta}_t\right), \quad (8)$$

where

$$\begin{aligned} \tilde{\mu}\left(Y(0), \tilde{Y}(t), X\right) &:= \frac{\beta_t \sqrt{\bar{\alpha}_{t-1}}}{1 - \bar{\alpha}_t} Y(0) + \frac{(1 - \bar{\alpha}_{t-1}) \sqrt{\alpha_t}}{1 - \bar{\alpha}_t} \tilde{Y}(t) + \\ &\quad \left(1 + \frac{(\sqrt{\bar{\alpha}_t} - 1)(\sqrt{\alpha_t} + \sqrt{\bar{\alpha}_{t-1}})}{1 - \bar{\alpha}_t}\right) f_\phi(X) \end{aligned}$$

and

$$\tilde{\beta}_t := \frac{1 - \bar{\alpha}_{t-1}}{1 - \bar{\alpha}_t} \beta_t. \quad (9)$$

$\bar{\alpha}_t$ ,  $\alpha_t$  and  $\tilde{\beta}_t$  can be directly calculated because  $\beta_t$ 's are constants predetermined by us. Consequently, we can generate  $\tilde{Y}(t-1)$  using (8) by incorporating  $\tilde{Y}(t)$ ,  $Y(0)$ , and  $f_\phi(X)$ . The generation process is expressed as follows:

$$\tilde{Y}(t-1) = \tilde{\mu}\left(Y(0), \tilde{Y}(t), X\right) + \sqrt{\tilde{\beta}_t} \epsilon_{t \rightarrow (t-1)}, \quad (10)$$

where  $\epsilon_{t \rightarrow (t-1)} \sim N(0, 1)$ , for  $t = T, \dots, 1$ . By repeating this process  $N$  times, we generate  $N$  pseudo samples.

However, in the reverse process, we do not possess  $Y(0)$ . So, we use the predicted  $Y(0)$  instead of directly using  $Y(0)$ . Specifically, by (6),

$$\mathbf{Y}(0) = \frac{1}{\sqrt{\bar{\alpha}_t}} \left( \mathbf{Y}(t) - (1 - \sqrt{\bar{\alpha}_t}) f_\phi(\mathbf{X}) - \sqrt{1 - \bar{\alpha}_t} \epsilon_{0 \rightarrow t} \right).$$

We use a deep neural network  $nn_\theta$  to approximate  $\epsilon_{0 \rightarrow t}$ . The loss function can be formulated as:

$$L = \mathbb{E}_{t, \mathbf{Y}(0), \mathbf{Y}(t)} \|\epsilon_{0 \rightarrow t} - nn_\theta(\mathbf{X}, \mathbf{Y}(t), f_\phi(\mathbf{X}), t)\|^2.$$

With the loss function, we can leverage optimization algorithms like Adam [39] to train the neural network  $nn_\theta$ , aiming to bring  $nn_\theta$  sufficiently close to  $\epsilon_{0 \rightarrow t}$ . Then, in the reverse process (10),  $Y(0)$  is replaced by its predicted value:

$$\begin{aligned} \hat{Y}^t(0) &= \frac{1}{\sqrt{\bar{\alpha}_t}} \left[ \tilde{Y}(t) - (1 - \sqrt{\bar{\alpha}_t}) f_\phi(X) \right. \\ &\quad \left. - \sqrt{1 - \bar{\alpha}_t} nn_\theta(X, \tilde{Y}(t), f_\phi(X), t) \right]. \end{aligned}$$

Refer to Figure 8 and Algorithm 1 for the detailed process and algorithm that illustrates the conditional diffusion model used to generate pseudo samples of  $Y|X$ .

## A.2 Comparative experiment

Table 5: The coverage rates and average lengths of different confidence intervals with confidence levels of 90% and 95%.

Methods	Coverage rate (90%)	Average length (90%)	Coverage rate (95%)	Average length (95%)
Linear quantile regression	95.1%	413.0	96.4%	452.4
Random forest quantile regression	80.0%	331.7	85.8%	381.9
Conformalized quantile regression	79.2%	251.2	84.3%	291.8
Ours	93.2%	317.0	95.1%	387.5

The proposed method constructs confidence intervals by directly learning the conditional distribution of  $Y|X$ . Besides, other commonly used methods for constructing confidence intervals include the quantile regression and the conformal prediction. So, we use the linear quantile regression [40], the random forest quantile regression [41], and the conformalized quantile regression [42] to construct confidence interval estimations, and compare the results with ours. Detailed results can be found in the Table 5, Figures 9, 10 and 11.

Table 5 reveals that the linear quantile regression produces relatively longer interval estimations, potentially leading to resource wastage. The average length of interval estimation provided by the random forest quantile regression is similar to ours, but this method fails to cover enough samples. The conformalized quantile regression yields notably short interval estimations, but its coverage rate is the lowest. Considering both the coverage rate and the average length, our approach has the most favorable performances.

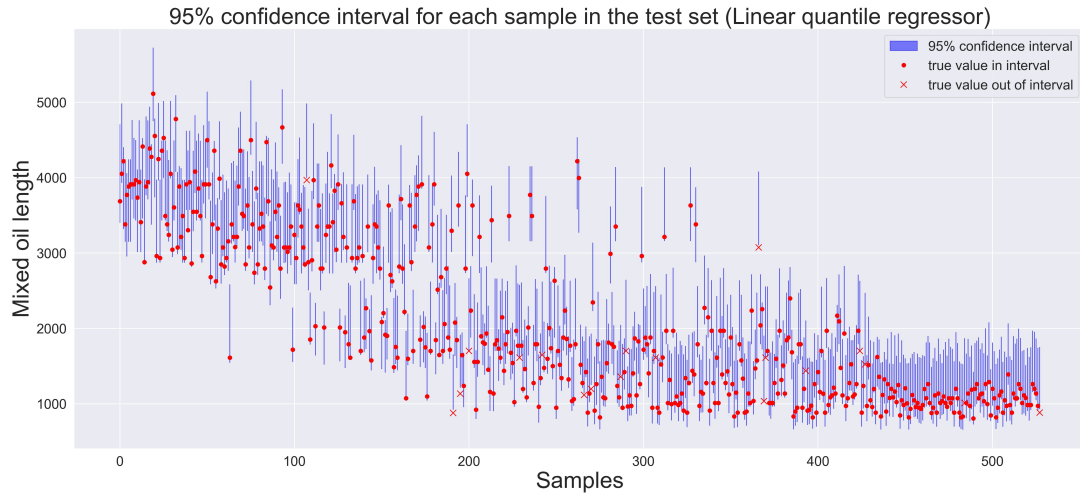
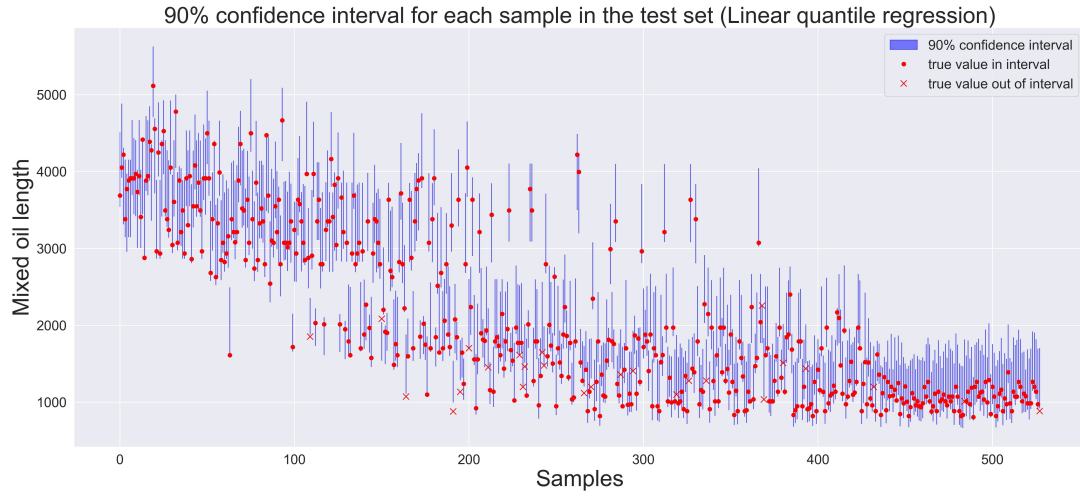


Figure 9: Interval estimations constructed by the linear quantile regression with confidence levels of 0.9 and 0.95. Coverage rate and average length of the intervals can be found in Table 5.

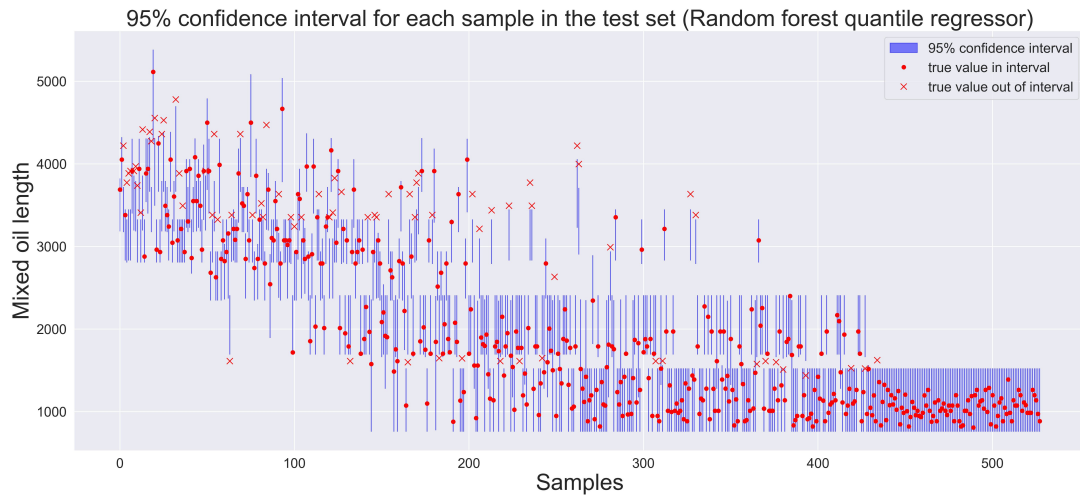
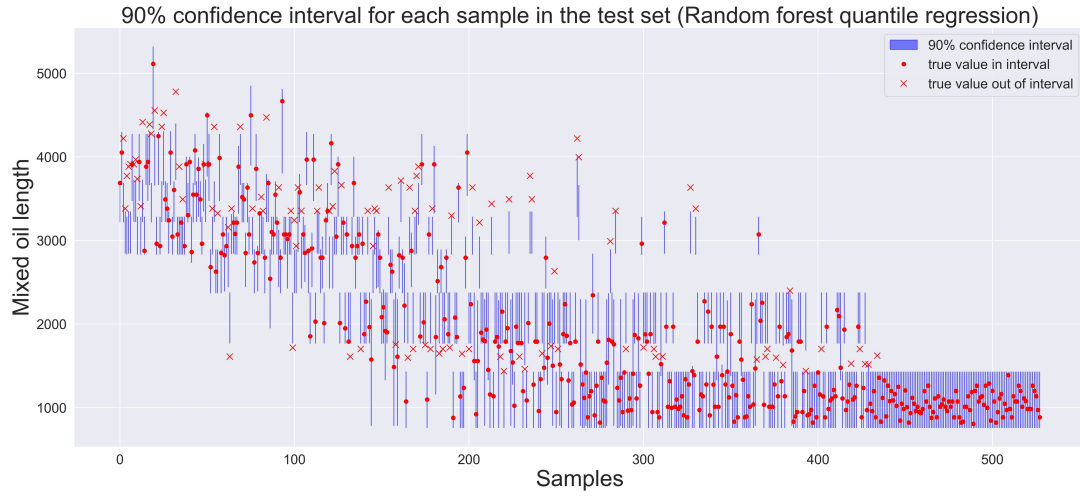


Figure 10: Interval estimations constructed by the random forest quantile regression with confidence levels of 0.9 and 0.95. Coverage rate and average length of the intervals can be found in Table 5.

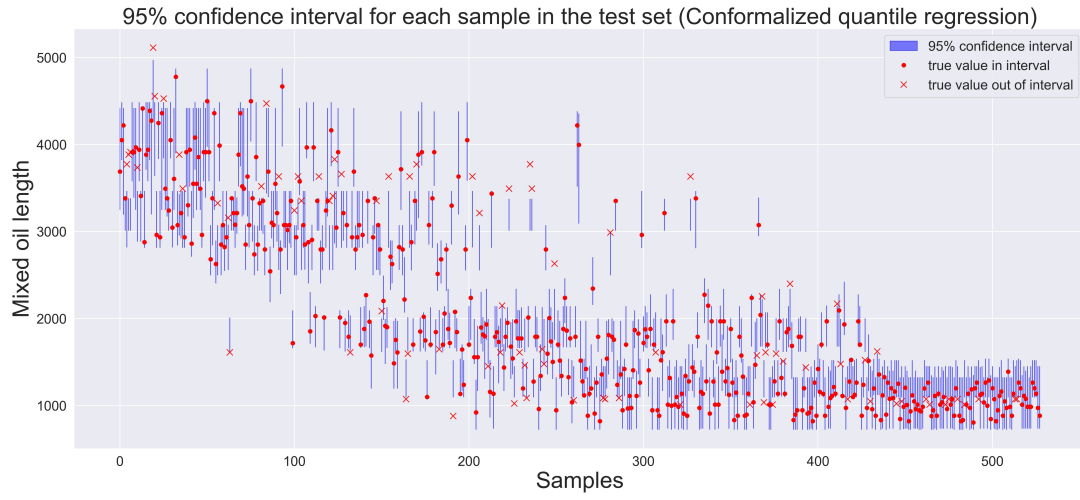
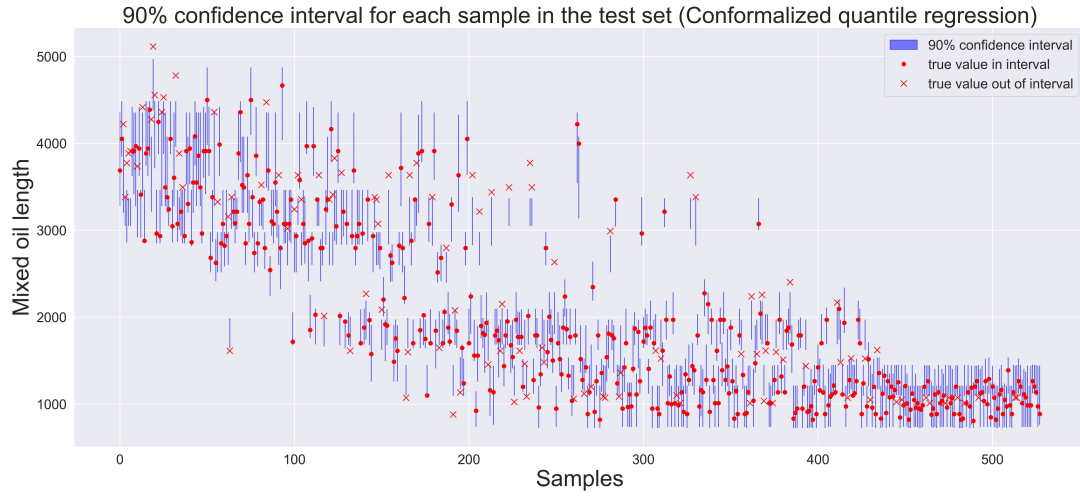


Figure 11: Interval estimations constructed by the conformalized quantile regression with confidence levels of 0.9 and 0.95. Coverage rate and average length of the intervals can be found in Table 5.